# INFLUENCE OF LOAD APPLICATION AND FIXTURE ON CHARACTERISTIC VALUES AT SHORT-TIME DYNAMIC COMPRESSION TESTING OF CARBON FIBER-EPOXY COMPOSITES

T. Schmack[1], D. Huelsbusch[2], R. Righi[1], J. Rausch[3], D. Roquette[3], G. Deinzer[1], F. Walther[2]

[1]Light Weight Center, N/EK-114, Audi AG, NSU-Straße 1, 74148 Neckarsulm, Germany
Email: tobias.schmack@audi.de, Web Page: www.audi.de
[2]Department of Materials Test Engineering (WPT), TU Dortmund University, Baroper Str. 303, 44227 Dortmund, Germany. Email: daniel.huelsbusch@tu-dortmund.de, Web Page: www.wpt-info.de
[3]Light Weight Center, N/EK-111, Audi AG, NSU-Straße 1, 74148 Neckarsulm, Germany
Email: julius.rausch@audi.de, Web Page: www.audi.de

**Keywords:** CFRP, compression strength, load application , material characteristic, strain rate

## Abstract

This study deals with the comparison of two fixtures to obtain strain rate-dependent properties of carbon fiber-reinforced plastics (CFRP) under axial compression. While the quasi-static method is mostly state of the art and covered in standards, dynamic high-speed testing of CFRP is very demanding in terms of testing procedure, test rig and failure mechanisms. This study contributes to the development of a new testing fixture by analyzing the influence of different load-transfer mechanisms on mechanical properties. In this context, unidirectional carbon fiber-reinforced epoxy prepreg under short-time dynamic compression is investigated. From experimental results it is evident that load application and specimen geometry affect the characteristic compression values. A significant difference in maximum compression strength was found between the two test fixtures applied.

## 1. Introduction

Lightweight structures have always been an issue in the design process of loadbearing components (e.g. car body development in automotive industry). For automotive parts legal crash load cases are of major importance when it comes to defining wall thickness and fiber orientation. In order to dimension parts and ensure vehicle crash safety, finite element crash simulations are performed. To optimize the prediction accuracy of the simulation, reliable mechanical data from dynamic testing are required. Hence, for this reason it is necessary to derive characteristic compression values from short-time dynamic testing.

In literature, limited information on methods for strain rate dependent compression testing are available. Existing studies show a large diversity in terms of testing methods and material combinations, thus not facilitating a general conclusion for an ideal test method. However, all studies show a significant strain rate dependence of fiber-reinforced plastics (FRP). The studies done by Körber [1,2] showed that the axial compression, the transverse compression and the in-plane shear material properties (Young's modulus, yield strength, and failure strength) increase with increasing strain rate. Similar behavior was found by using a falling weight impact tower. In detail, stress-strain curves straighten with the increase of strain rate [3]. In contrast to measurements using a split-Hopkinsson pressure bar [1], higher failure strengths were observed. Amijima and Fujii [4] studied the effects of strain rate on compression strength of unidirectional glass/polyester and woven glass/polyester composites ($10^{-3}$ to $10^{3}$ $s^{-1}$). Moreover, they found that the compression strength of both types of composites increased with strain rate. The increase in strength was also shown to be higher for the woven composites than for the unidirectional ones. Axial compression tests on a glass fiber reinforced plastics were carried out by Shokrieh and Omidi [5]. This publication shows that

Excerpt from ISBN 978-3-00-053387-7

material hardening appears with increasing strain rate. It was found that both, compression strength and compression modulus increase with increasing strain rate. In addition, the results show that the compression strain to failure is generally independent of strain rate. In this study a servo-hydraulic cylinder with a specially developed compression device for the rectangular flat specimens was used. Hsiao and Daniel investigated the influence of two different load transmissions on the compression strength of thick unidirectional composites [3]. The pure head loading shows due to crushing effects near the load transmission a much smaller compression strength in comparison to the Northwestern University method (NU-method: combination of head and shear load transmission). A wide range of testing of the strain rate dependent material behaviour of thermoplastic composites was carried out by Schmidt and Endemann [6]. In this context, a fixture for short-time dynamic compression testing was developed.

The results presented in this study contribute to the recent work in the field of strain rate-dependent testing, focussing on the effect of the load transfer into the specimen and its effect on the results, i.e. compression strength and Young's modulus.

## 2. Experimental

### 2.1. Materials selection and specimens preparation

A commercial high-modulus carbon fiber (T700, Toray) with a tensile strength of 4,900 MPa was used as a part of epoxy-based prepreg system (DT120, Delta-Tech, areal weight 150g/m$^2$) [7,8]. Unidirectional laminates with different thicknesses (10 layer: thickness = 2 mm, 18 layers: thickness = 3.2 mm) were manufactured using the autoclave process. The curing of the laminates followed the suppliers recommendations for autoclave processing [7].

High quality of the manufactured laminates was required; therefore several quality inspections were performed. The first step is the thickness measurement using a Kroeplin IP 67. The thickness is measured in nine different positions. Furthermore the resins curing degree (CD) is checked by differential scanning calorimetry (DSC) (Mettler Toledo DSC 1) testing three separate positions of the laminate, taking one measurement at each position. The fiber volume content (FVC) is determined by a density measurement using an uplift scale (Mettler Toledo) in three separate positions of the laminate, taking three measurements at each position.

For sample preparation in the first step, the initial plates are cut in smaller rectangulars by waterjet cutting so that the glass fiber-reinforced plastic (GFRP) tabs can then be bonded. The bonding surface of the plates is roughened through sandblasting. The GFRP tabs were applied with 2-component-epoxy adhesive on to the sandblasted surface. The final cut of the desired width was achieved by means of a water-cooled diamond precision saw. Two different specimen geometries were manufactured.

Figure 1 shows the two different specimen geometries, which differ in terms of thickness, length and width. These changes were necessary because the two testing devices are each designed for the respective individual geometries.

For elongation measurement a stochastic greyscale pattern is applied to the specimen. Specimen (A) in Fig. 1 obtains the pattern in the gauge area, whereas specimen B receives the pattern only at the front face due to the clamping. For specimen (B), in addition to the greyscale pattern, strain gauges are applied in the gauge area at the front and at the back of the specimen.

Excerpt from ISBN 978-3-00-053387-7

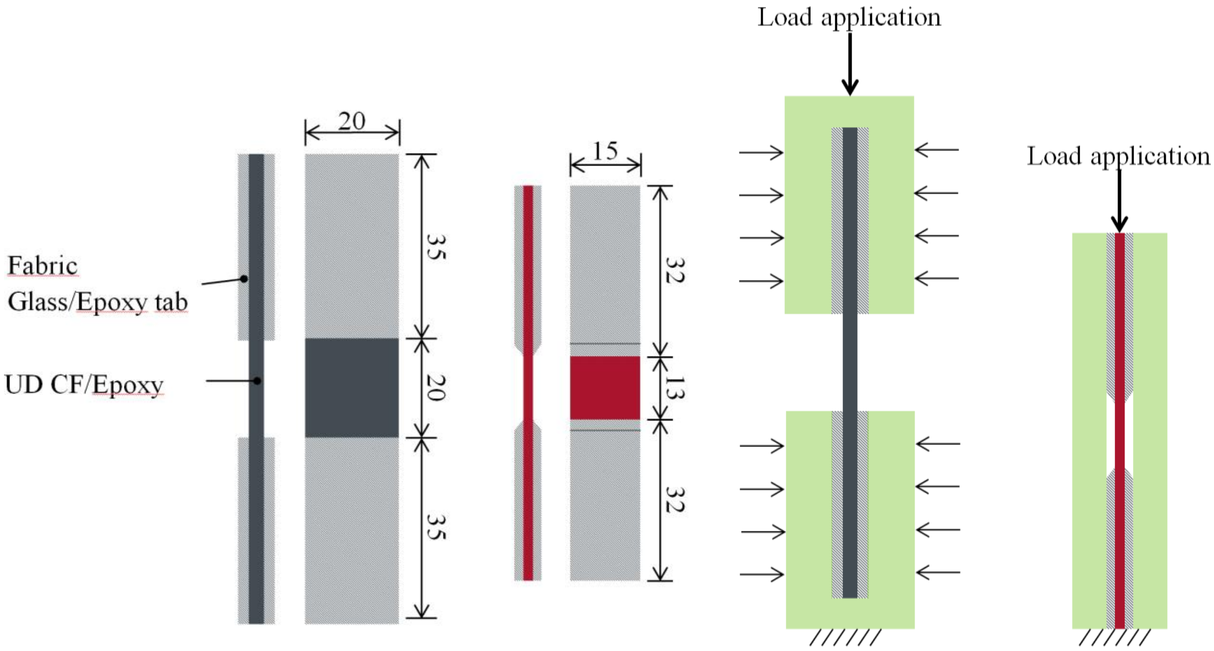


**Figure 1.** Specimen geometries. Differing in terms of thickness, (A) = 3.2 mm and (B) = 2 mm. Different concepts of load transfer, (C) combined shear-end loading (NU-method) and (D) pure end loading.

### 2.2 Testing machine and equipment

Two different fixtures with different load transmission methods were used, shown schematically in Fig. 1. In both cases the initial impact energy is produced by a servo-hydraulic cylinder and the force is measured using a piezoelectric measuring cell.

Figure 1 (C) illustrates how the force application is realized using a combination of head and shear load transmission. The initial impact energy is introduced smoothly by a cone/sleeve mechanism. The specimen is held in the upper and lower clamping jaws. This setup is similar to the setup used in [6]. The fixture consists of a four pillar guide to ensure uniaxial load application to avoid bending forces which lead to a stability failure, buckling.

The load transmission principle by pure head impact is shown in Fig. 1 (D). A key aspect of this method is not to clamp the specimen, but simply support it on the sides. The support is achieved using a honeycomb structure which has a much smaller stiffness in longitudinal direction than in transverse one.

## 3. Results and discussion

For quality assurance aspects, the testing plates were characterized by FVC and CD. The results are listed in Table 1.

Excerpt from ISBN 978-3-00-053387-7

**Table 1.** Quality assurance by DSC and density measurement

| Plate | Spot | FVC (%) | Ø FVC (%) | CD (%) | Ø CD (%) |
|---|---|---|---|---|---|
| | A1 | 54.89 ± 1.02 | | 97.45 | |
| A | A2 | 52.82 ± 0.59 | 53.49 ± 1.21 | 95.94 | 96.90 ± 0.68 |
| | A3 | 52.76 ± 0.28 | | 97.32 | |
| | B1 | 52.19 ± 0.34 | | 98.78 | |
| B | B2 | 51.85 ± 0.43 | 52.01 ± 0.41 | 99.15 | 99.00 ± 0.16 |
| | B3 | 51.98 ± 0.40 | | 99.06 | |

### 3.1 Combined shear/end loading fixture

Figure 2 illustrates the raw data obtained from the testing described in Fig. 1 (C). The linear characteristic of the stress-strain curve is atypical for dynamic measurements of this type. Usually, oscillations occur in the system due to the forces being introduced by an impulse which superimposes the force signal [9–11]. Through changes in the construction, these superimpositions were successfully reduced to a minimum.

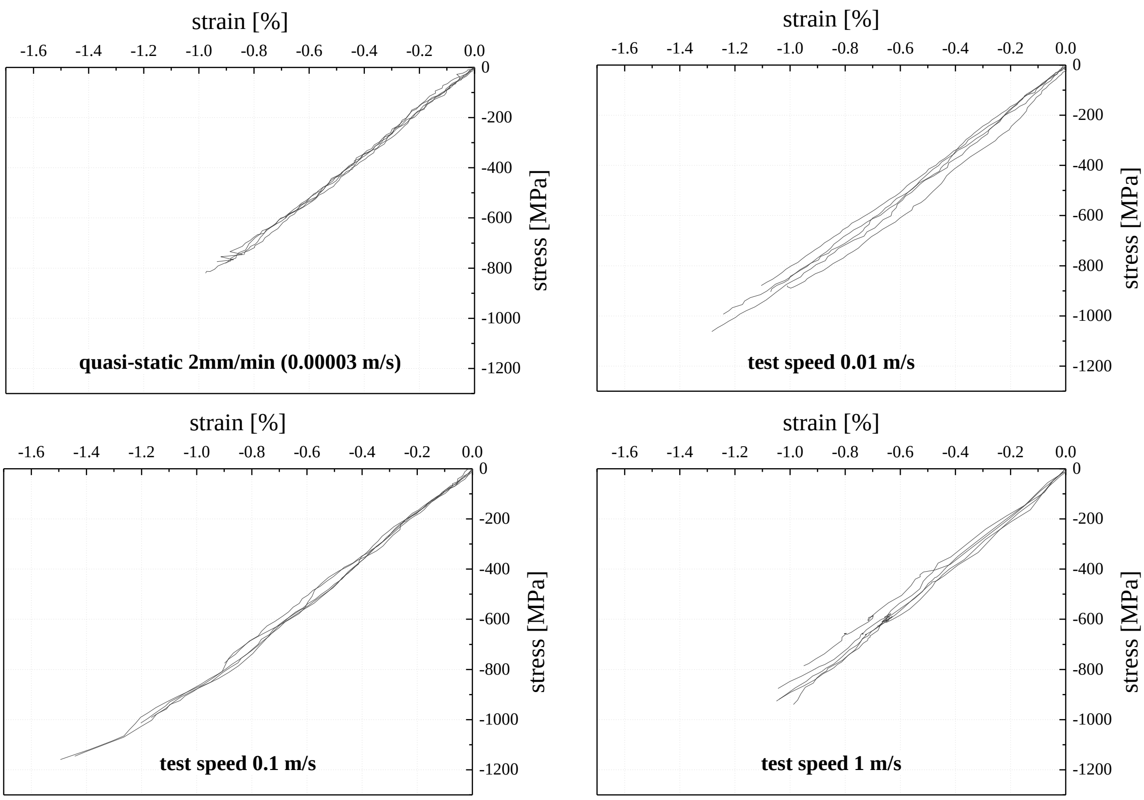


**Figure 2.** Quasi-static and dynamic stress-strain curves for unidirectional carbon/epoxy composite under combined shear/end loading (Fig. 1 (C))

The analysis of the raw data concerning compression strength is plotted in Fig. 3. In principle the typical strain rate dependent material characteristic, like in literature [2,3,5,12], was measured. The increasing compression strength is consistent from static up to strain rate of about 1.37 $s^{-1}$. At strain rate 3.5 $s^{-1}$ a significant decrease of mean compression strength from 1101 to 911 MPa (17.25%) was obtained.

Excerpt from ISBN 978-3-00-053387-7

To exclude possible material defects or an influence of the testing rig, specimen geometry B (Fig. 1(B)) was tested with the corresponding testing speed of 1 m/s. The results of these tests are visualized in Fig. 3, and are the major findings of this study. The specimen geometry is an important parameter; by reducing the gauge length from 20 to 13 mm a significant increase of compression strength was obtained. The observed effect could be related to smaller gauge length which has an influence on global and local buckling of the specimen. These critical buckling modes destabilize the specimen and reduce the effective cross-section [13].

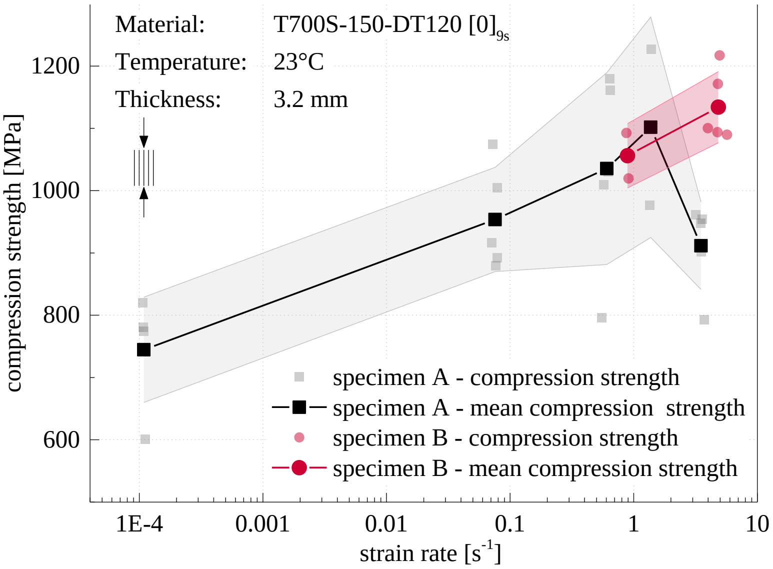


**Figure 3.** Static and dynamic compression strength of specimens (A)/(B) under combined shear/end loading (NU-method)

The typical characteristic of the failure mechanisms of an unidirectional composite under compression loading is given in Fig. 4. The pictures were magnified with the help of a CT (General Electrics E Phoenix Nanotom M). The stability failure initiated by a so-called ‘kink band’ (Fig. 4 (A)) which shows a side face view of the specimen. This kink band can be understood as buckling of the fibers at the micro-level [14]. After local exceeding of matrix compression strength, the matrix support fails and initiates the micro-buckling of the fiber. For that reason the strain rate-dependent characteristic of the laminate is related to matrix properties. Furthermore, as shown in Fig. 4 (B), the fracture occurs at an angle of 15 degrees. This angle indicates compression shear failure of the laminate transverse to the fiber orientation [15].

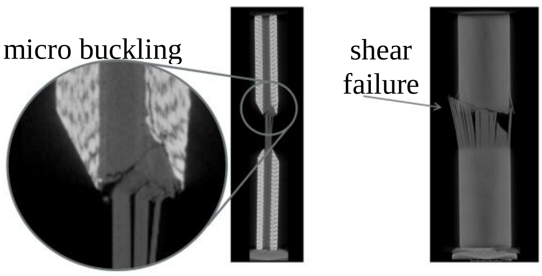


**Figure 4.** CT scan. (A) Fracture characteristic (kink band) of an unidirectional laminate due to axial compression loading, (B) section view with hidden tabs

### 3.2 Pure end loading fixture

In contrast to combined load introduction by shear/end loading, pure end loading requires accurate specimen preparation concerning plane parallelism of the end surfaces and tabs. Local force peaks

Excerpt from ISBN 978-3-00-053387-7

initiate local failure which leads to a reduction of the overall compression strength [3]. In total six specimens showed this kind of failure and have therefore been removed as outliers from the test results. However, the small variance of the compression strength shown in Fig. 5 is an indicator for a reliable testing method. The quantitative increase of 72% of compression strength from static (784 MPa) to strain rates of 123 $s^{-1}$ (1348 MPa) is higher than noted in literature [2,3,5,12].

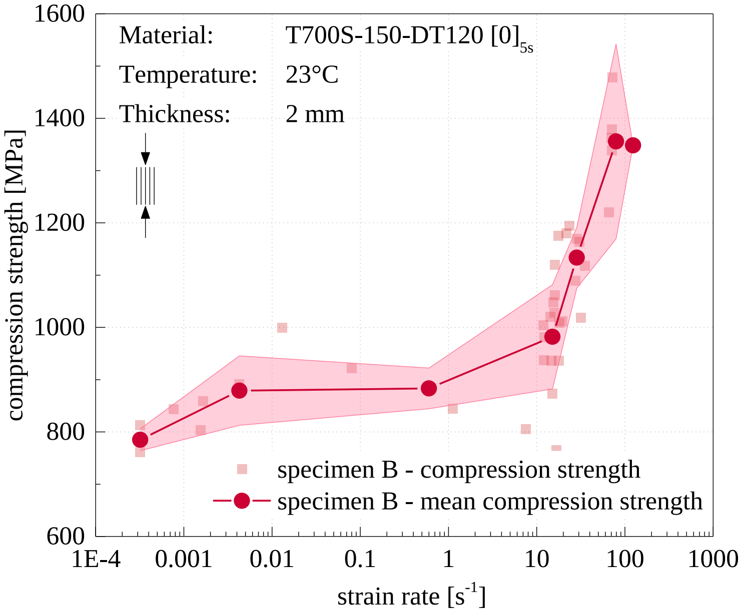


**Figure 5.** Static and dynamic compression strength of specimen (B) under pure end loading

### 3.3 Comparison of load application concept (A) and (B) end loading only

The dynamic elastic modulus reflects the viscoelastic characteristic of the tested material configuration and is given in Fig. 6. Hence, the initial modulus determination is established by secand modulus in an area of 0.1 to 0.3% elongation.

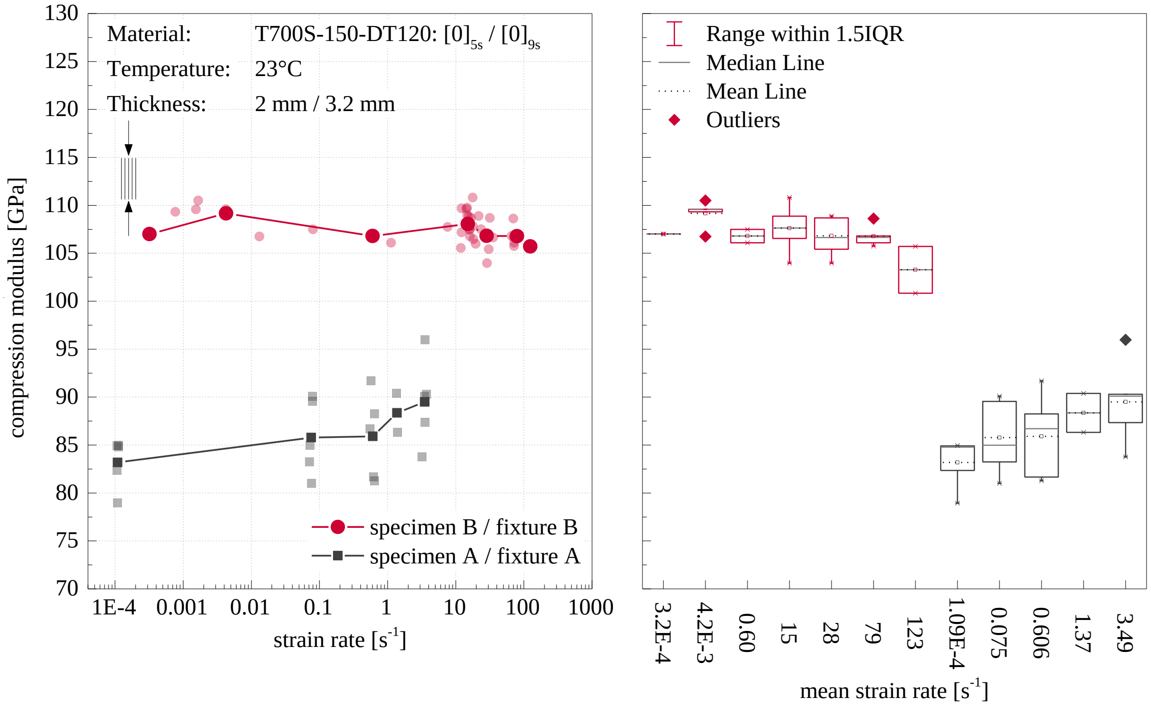


**Figure 6.** Static and dynamic initial modulus from two different loading concepts

Excerpt from ISBN 978-3-00-053387-7

The large scatter of the determined characteristic values is shown by the error bars of the averaged individual measurements. This deviation could be the result of the method of secante modulus. The overlap of the confidence intervals in the box plot (Fig. 3 (B)) indicates that there is insufficient significance of the measured parameters which agrees with literature values [16]. However, the average increase of the modulus of 10% (specimen A/NU-method) needs to be taken into account, but may be related to influences of inertia masses while measuring.

Figure 7 shows the compression strength of the two different load transfer principles. The combined shear/end loading method shows compression strength increases with increasing strain rate. This effect is plausible based on the similar results obtained by Hsiao on his studies of thick laminates [3].

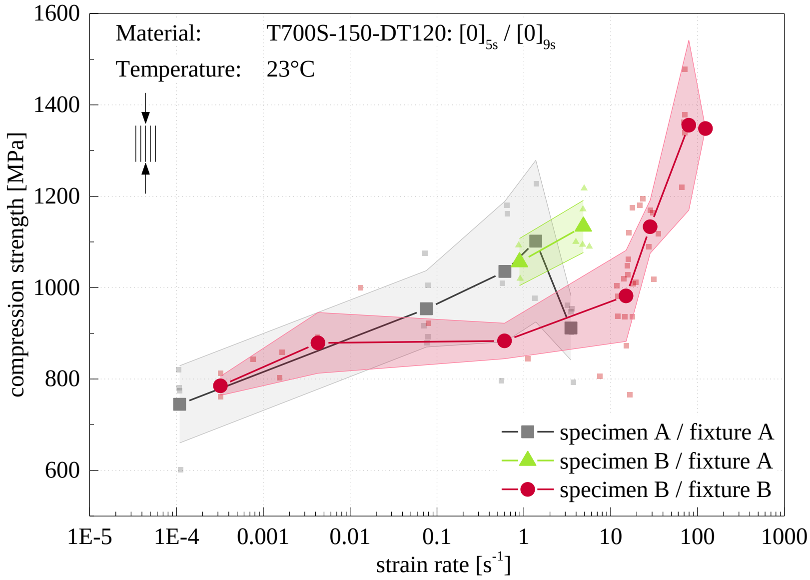


**Figure 7.** Static and dynamic compression strength of the investigated specimen geometries and loading concepts

## 4. Conclusion

The results obtained using the NU-method and pure end loading in a servo-hydraulic testing machine corroborate both the predicted and well known increase of longitudinal compression strength of CFRP with increasing strain rate. Due to high variance of initial modulus no significant influence of increasing strain rate is concluded. The fracture characteristic of kink band and shear fracture agree to described phenomena in literature. However, the comparison of results from the two different loading concepts shows a major difference in initial modulus, compression strength and variance. Furthermore, the specimen geometry and testing speed show an influence on compression strength. The significant drop in compression strength at the test speed of 1 m/s and the established hypothesis of critical buckling modes are considered as important parameters for further investigations. In this context the influence of specimen geometry is detected as to be responsible for this effect. In a broader context all of these parameters should be optimized and investigated in additional research regarding a reliable material characteristic determination. The goal is to describe the laminate characteristics as accurately and realistically as possible so that they may be used in simulation models.

## Acknowledgments

This research was supported by Dipl.-Ing. Martin Holzapfel (DLR Stuttgart) and Dr.-Ing. Henrik Schmidt (BASF). I would like to thank both partners for the open and constructive discussions. I would like to show my special gratitude to Dipl. Ing. (FH) Harald Kraft (DLR Stuttgart) for sharing with me his decades of experience and knowledge in the field of materials testing.

## References

[1] H. Koerber, J. Xavier and P.P. Camanho, High strain rate characterisation of unidirectional carbon-epoxy IM7-8552 in transverse compression and in-plane shear using digital image correlation, *Mechanics of Materials* **42** (2010), 1004–1019.

[2] H. Koerber and P.P. Camanho, High strain rate characterisation of unidirectional carbon–epoxy IM7-8552 in longitudinal compression, *Composites Part A: Applied Science and Manufacturing* **42** (2011), 462–470.

[3] H.M. Hsiao and I.M. Daniel, Strain rate behavior of composite materials, *Composites Part B: Engineering* **29B** (1998).

[4] F.T. Amijima S, *Compression strength and fracture characteristics of fiber composites under impact loading*, Paris, 1980.

[5] M.M. Shokrieh and M.J. Omidi, Compression response of glass–fiber reinforced polymeric composites to increasing compression strain rates, *Composite Structures* **89** (2009), 517–523.

[6] H. Schmidt and U.M. Endemann, Improved testing of continuous fiber-reinforced plastics: taking into account the influence of strain rate in characterizing fiber-reinforced polymer composites, *Kunststoffe international* **3/2015** (2015), 12–17.

[7] Delta-Tech S.p.A., Technical Data Sheet: Delta preg t700 dt120, http://www.delta-tech.it/download.php?f=pdf/2015/DT120-MatrixTDS-10.pdf, accessed 13 April 2016.

[8] Toray carbon fibers America, Inc., Data sheet: Toray T700S, http://www.toraycfa.com/pdfs/T700SDataSheet.pdf, accessed 13 April 2016.

[9] J.P. Hessling, Models of dynamic measurement error variations of material testing machines, *Mechanical Systems and Signal Processing* **23** (2009), 2510–2518.

[10] R. Kumme, Investigation of the comparison method for the dynamic calibration of force transducers, *Measurement* **23** (1998), 239–245.

[11] R. Kumme, O. Mack, B. Bill, Ch. Gossweiler, H. R. Haab, The dynamic calibration of piezoelectric force measuring devices, *VDI Berichte 1685* (2002), 161–172.

[12] H.M. Hsiao, I.M. Daniel and S.C. Wooh, A new compression test method for thick composites, *Journal of Composite Materials* **29** (1995), 1789–1806.

[13] N. Feindler, *Charakterisierungs- und Simulationsmethodik zum Versagensverhalten energieabsorbierender Faserverbundstrukturen*, Technische Universität München, 2012.

[14] P. Berbinau, C. Soutis and I.A. Guz, Compression failure of 0° unidirectional carbon-fiber-reinforced plastics (CFRP) laminates by fibre microbuckling, *Composites Science and Technology* **59** (1999), 1451–1455.

[15] Rosen, Mechanics of composite strengthening, *Fibre composite materials* (1965), 37–75.

[16] I.M. Daniel, B.T. Werner and J.S. Fenner, Strain-rate-dependent failure criteria for composites, *Composites Science and Technology* **71** (2011), 357–364.

Excerpt from ISBN 978-3-00-053387-7